Deposition fluxes and fate of polycyclic aromatic hydrocarbons in the Yangtze River estuarine–inner shelf in the East…

Article · March 2013

DOI: 10.1029/2012GB004317

CITATIONS
24

READS
56

5 authors, including:

Tian Lin
Chinese Academy of Sciences
53 PUBLICATIONS **1,108** CITATIONS
SEE PROFILE

Limin Hu
33 PUBLICATIONS **730** CITATIONS
SEE PROFILE

Zhigang Guo
Nanjing Normal University
101 PUBLICATIONS **2,432** CITATIONS
SEE PROFILE

Gan Zhang
Chinese Academy of Sciences
421 PUBLICATIONS **12,766** CITATIONS
SEE PROFILE

Deposition fluxes and fate of polycyclic aromatic hydrocarbons in the Yangtze River estuarine-inner shelf in the East China Sea

Tian Lin,[1] Limin Hu,[2] Zhigang Guo,[1,3] Gan Zhang,[4] and Zuosheng Yang[3]

Received 9 February 2012; revised 30 October 2012; accepted 6 November 2012; published 31 January 2013.

[1] Surface sediments were obtained from a matrix of 76 sample sites in the inner shelf mud belts of the East China Sea (ECS) for a comprehensive study of the distribution, composition, deposition flux, and fate of polycyclic aromatic hydrocarbons (PAHs). The sampling sites covered an area of ~80,000 km^2 extending ~1000 km from the mouth of the Yangtze River to the Min River in the inner shelf. The total deposition flux of the 16 USEPA priority PAHs (16 PAHs) of the Yangtze estuarine-inner shelf was estimated to be 152 t/yr, accounting for ~38% of the total annual input of the 16 PAHs into the ECS. This indicates that the Yangtze estuarine-inner shelf is one of the largest sinks of land-based PAHs in the world. Principal component analysis indicated that the 16 PAHs in the northern Yangtze estuarine mud area were mostly phenanthrene while shifting to high-molecular-weight PAHs in the southern Min-Zhe coastal mud area. The positive matrix factorization model revealed that the deposition flux of low-molecular-weight (LMW) PAHs decreased from north to south, most likely due to the mass transfer between the resuspended sediments triggered by the East Asian monsoon and the water columns, as the resuspended sediments are transported southward. This release of LMW PAHs from the sediments to the water columns could become an important secondary PAH source in ECS.

Citation: Lin, T., L. Hu, Z. Guo, G. Zhang, and Z. Yang (2013), Deposition fluxes and fate of polycyclic aromatic hydrocarbons in the Yangtze River estuarine-inner shelf in the East China Sea, *Global Biogeochem. Cycles*, *27*, 77–87, doi:10.1029/2012GB004317.

1. Introduction

[2] Polycyclic aromatic hydrocarbons (PAHs) are toxic and carcinogenic and are ubiquitous in the environment. They are mainly released from the incomplete combustion of fossil fuels, municipal wastes, and biomass [*Yunker et al*., 2002], the spills of petroleum-derived products, and the diagenesis of organic matter in the anoxic environment [*Lima et al*., 2005; *Berrojalbiz et al*., 2011]. In the estuarine-coastal environment, river discharge, surface runoff, and the sedimentary process are more influential on the distribution and behavior of persistent organic pollutants, including PAHs, than atmospheric deposition [*Greenfield and Davis*, 2005; *Hu et al*., 2011; *Lin et al*., 2011]. There have been several studies focusing on the fate of atmospherically deposited PAHs and the factors that influence the distribution and composition of the PAHs in coastal areas [*Arzayus et al*., 2001; *Tsapakis et al*., 2003, 2006]; however, fluxes, transport, and fate of PAHs in large river-influenced seas, such as the East China Sea (ECS), remain scarcely documented. It is estimated that the annual flux of the 16 USEPA priority PAHs (16 PAHs) from the Yangtze River to the sea was 232 t, significantly higher than the Yellow River (70.5 t) in north China and the Pearl River (33.9 t) in south China [*Wang et al*., 2007].

[3] The ECS is a marginal sea greatly influenced by the Yangtze (Figure 1). As the fifth largest river in water discharge and the fourth largest in sediment discharge in the world (Table S1), the Yangtze is one of the largest contributors of terrestrial sediments to the western Pacific shore [*Wang et al*., 2011]. The drainage basin of the Yangtze is ~1.94×10^6 km^2, accounting for ~20% of the area of the Chinese mainland with 400 million inhabitants [*Yang et al*., 2006; *Bianchi and Allison*, 2009; *Chu et al*., 2009]. The total annual average in sediment discharge by several other major local rivers (including the Qiantang River, Ou River, and Min River) amounts to only ~4% of the Yangtze's annual sediment load [*Liu et al*., 2007; *Chu et al*., 2009].

[4] The discharged sediments and associated pollutants are mostly trapped in the Yangtze River Estuary (YRE) and the inner shelf of ECS, owing to the net effects of the shear forces of the coastal currents [*Milliman et al.*, 1985; *Liu et al*., 2006, 2007; *Bianchi and Allison*, 2009] (Figure 1). In the June–October flood season, the Yangtze discharges ~87% of its mean annual sediments [*Guo et al*., 2007], while the northward Zhejiang-Fujian coastal current (ZFCC) is weak

All supporting information may be found in the online version of this article.

[1]Department of Environmental Science and Engineering, Fudan University, Shanghai, China.
[2]Key Laboratory of Marine Sedimentology and Environmental Geology, First Institute of Oceanography, State Oceanic Administration, Qingdao, China.
[3]College of Marine Geosciences, Ocean University of China, Qingdao, China.
[4]State Key Laboratory of Organic Geochemistry, Guangzhou Institute of Geochemistry, Chinese Academy of Sciences, Guangzhou, China.

Corresponding author: Z. Guo, Department of Environmental Science and Engineering, Fudan University, Shanghai 200433, China. (guozgg@fudan.edu.cn)

0886-6236/13/2012GB004317

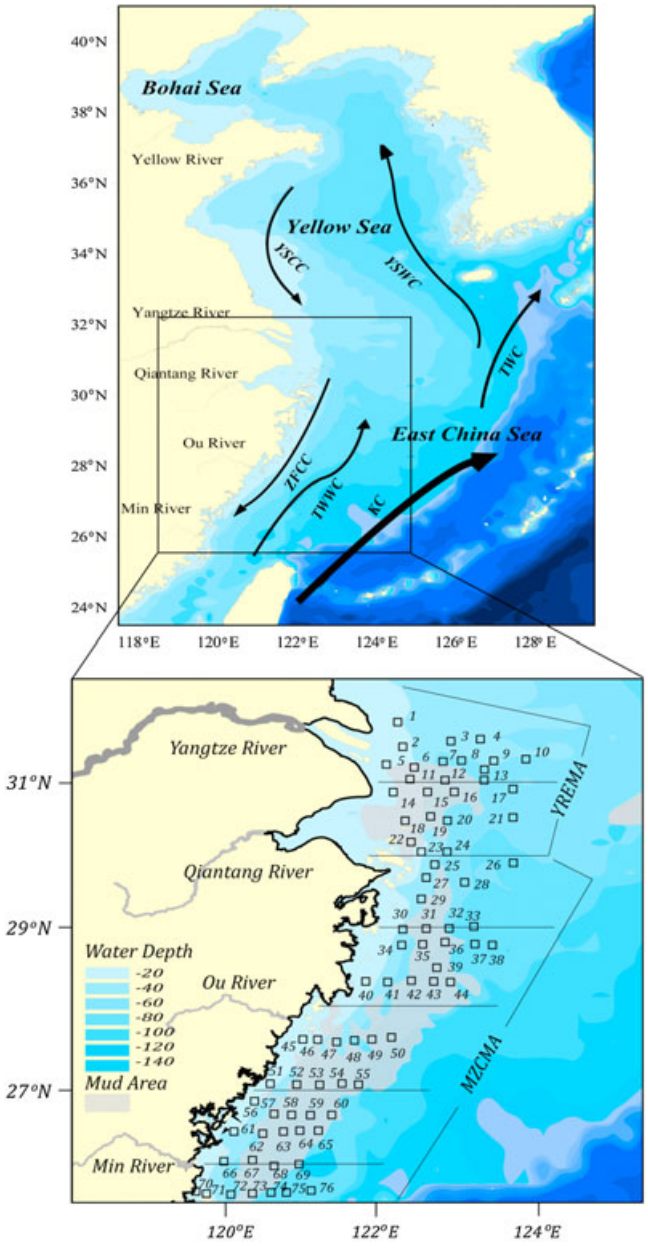

Figure 1. Map of sampling sites in YREMA and MZCMA. KC, Kuroshio current; TWC, Tsushima warm current; YSCC, Yellow Sea coastal current; YSWC, Yellow Sea warm current. Circulation system and mud areas (in light gray) are after *Liu et al*. [2007].

and the Taiwan Warm Current (TWWC) is strong due to the prevailing southeast monsoon. This leads to the accumulation of the Yangtze-derived sediments in the subaqueous delta and estuarine system, forming the YRE mud area (YREMA) [*Guo et al*., 2007; *Liu et al*., 2006, 2007]. In winter, strong wind-induced waves readily resuspend the newly deposited sediments in YREMA. The resuspended fine particles are transported southward along the inner shelf by the southward ZFCC driven by the East Asian monsoon and are constrained to the inner shelf of ECS owing to the obstruction of the northward-flowing strong TWWC, thus forming the Min-Zhe coastal mud area (MZCMA), an elongated mud wedge 40–60 m under the water extending ~1000 km from the Yangtze mouth to the Taiwan Strait [*Liu et al*., 2006, 2007]. Approximately 40% of the Yangtze-derived sediments is deposited in the YRE north of 30°N, while 32% is believed to be accumulated in the MZCMA [*DeMaster et al*., 1985; *Liu et al*., 2007].

[5] When the sediments initially deposited in YREMA are resuspended by the winter East Asian monsoon, and the PAHs associated with the sediments may be mass transferred to the water columns according to their respective solubility, while the particles are transported and eventually redeposited, resulting in a redistribution of the PAHs along the inner shelf of ECS in both phases. Therefore, the Yangtze estuarine-inner shelf is a scientifically unique and ideal site to study and estimate the land-sea PAH deposition flux, and to examine the role of hydrodynamic sedimentary processes on the partitioning and fate of PAHs in the sediments.

2. Materials and Methods

2.1. Sampling

[6] The sampling sites are shown in Figure 1. Most samples were collected from the mud areas. Surface sediment samples (0–3 cm) were collected using a stainless steel box corer during two cruises in 2006 and 2007. Sediment samples wrapped in aluminum foil were stored at –20°C until analysis.

2.2. Analysis of PAHs, Total Organic Carbon (TOC), and Sediment Grain Size

[7] The PAH analysis procedure and QA/QC followed that described by *Lin et al*. [2011]. The 16 PAHs measured were naphthalene (NAP), acenaphthylene (AC), acenaphthene (ACE), fluorine (FL), phenanthrene (PHE), anthracene (ANT), fluoranthene (FLU), pyrene (PYR), benz[a]anthracene (BaA), chrysene (CHR), benzo[b]fluoranthene (BbF), benzo[k]fluoranthene (BkF), benzo[a]pyrene (BaP), indeno[1,2,3-cd]pyrene (IP), dibenz[a,h]anthracene (DBA), and benzo[ghi]perylene (BghiP). The average surrogate recoveries were $71.5 \pm 11.2\%$ for NAP-d_8, $70.0 \pm 9.8\%$ for ACE-d_{10}, $86.2 \pm 12.3\%$ for PHE-d_{10}, and $90.1 \pm 10.5\%$ for perylene-d_{12}, respectively. Nominal detection limits for the individual PAH ranged from 0.2 to 2.0 ng/g (dry weight) for 10 g of sediments. In this study, all compounds were detected with the detection frequencies of close or equal to 100% for the measured samples, except AC (65%) and DBA (81%) (see Table S2). The relative precision of paired duplicated samples was below 15% (n = 8), and the targeted compounds were not detected in procedural blank (n = 8).

[8] The analytical methods of TOC and sediment grain size were according to *Hu et al*. [2009]. Replicate analysis of one sample (n = 8) gave a precision of ±0.02 wt% for TOC. For the sediment grain size, the relative error of the duplicate samples was less than 3% (n = 6). The particle sizes were >63 μm for sand, 4–63 μm for silt, and <4 μm for clay.

2.3. Principal Component Analysis (PCA) and Positive Matrix Factorization (PMF)

[9] Before the analysis, undetectable values (null values) were replaced by one half of the method detection limit.

Un-normalized concentrations of the 16 PAHs of the 76 sediment samples were used in the PCA analysis. SPSS (SPSS Inc., Chicago, Ill.) was applied to extract the principal components (PCs) based on the correlation matrix. The PCs were that eigenvalues >1 were considered to be factors for further discussion.

[10] PMF is a PCA-based receptor model with non-negative constrains that involves the solution of quantitative source apportionment equations by oblique solutions in a reduced dimensional space. Detailed concept and application of PMF source apportionment are described in the EPA PMF 3.0 Fundamentals & User Guide (www.epa.gov/heasd/products/pmf). In principle, the PMF model is based on the following equation:

$$Xij = \sum_{k=1}^{p} Aik\ Fkj + Rij \quad (1)$$

where Xij is the concentration of the jth congener in the ith sample of the original data set, Aik is the contribution of the kth factor to the ith sample, Fkj is the fraction of the kth factor arising from congener j, and Rij is the residual between the measured Xij and the estimated Xij using p principal components.

$$Q = \sum_{i=1}^{n}\sum_{j=1}^{m}\left(\frac{Xij - \sum_{k=1}^{p} Aik\ Fkj}{Sij}\right)^2 \quad (2)$$

where Q is the weighted sum of squares of differences between the PMF output and the original data set. One of the objectives of PMF analysis is to minimize the Q value. Sij is the uncertainty of the jth congener in the ith sample of the original data set containing m congeners and n samples.

[11] Uncertainty file should be provided in the model as an estimate of the confidence level for each value. In this study, an uncertainty of 20% was adopted based on the results from regularly analyzing the standard reference material [*Mai et al.*, 2001]. PMF modeling was performed with 3 to 6 factors each individually initialized with different starting points. The 3-factor solution produced a Q value of 4348, very close to the theoretical value of 4556. Using three factors, the fit between the modeled and the measured concentrations yielded $R^2 = 0.69$–0.92. Although lower Q values could be obtained with 4 to 6 factors, adding more factors resulted in no substantial improvement in the ability to interpret the factor profiles. The 3-factor model was thus determined to be adequate in this study.

3. Results and Discussion

3.1. Sediment Grain Size and TOC

[12] The sediments in the inner shelf of ECS consisted largely of silt and clay with a median grain size of 6.87 Φ (Table S3). The silt and clay contents were 16–83 and 8–36%, respectively, and the average mud (sum of the two)

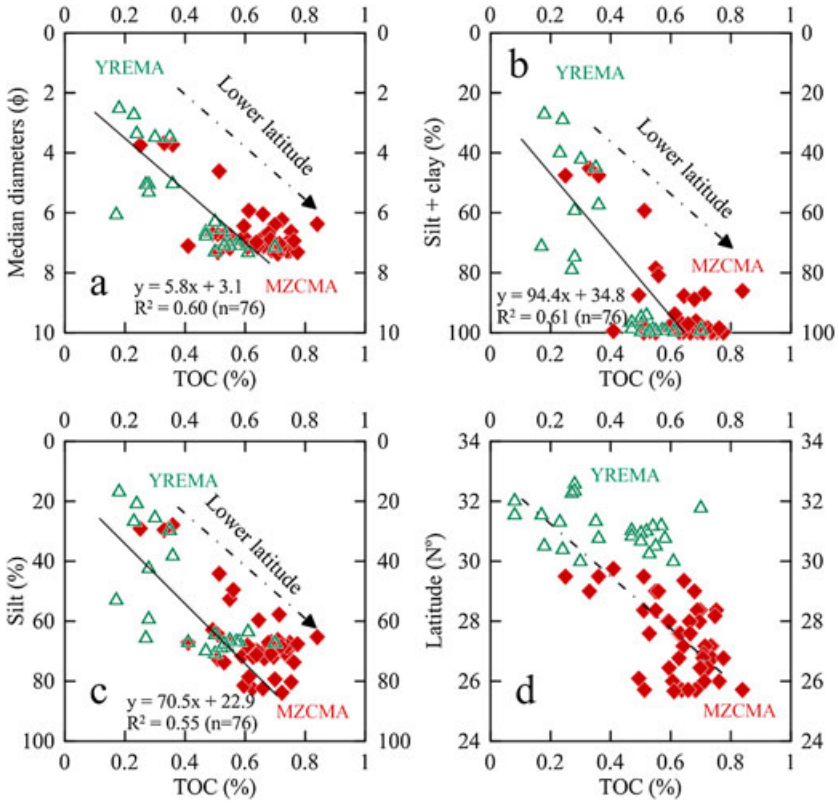

Figure 2. Correlations of TOC contents and median diameters (Φ) (a), silt + clay proportions (b) and silt proportions (c) and latitudinal distribution of TOC (d) in the sediments of the Yangtze estuarine-inner shelf of ECS.

content was 89 ± 18%. There was a slight increasing trend of the mud constituent along the coast southward from the YRE (Figure 2). TOC in YREMA ranged from 0.17 to 0.70% (dry weight) of the sediments and the mean was 0.42 ± 0.15%, lower than the 0.66 ± 0.08% in MZCMA. The TOC distribution also showed an increasing trend from the north to the south (Figure 2). There was a good positive correlation between TOC and the median grain size ($r^2 = 0.60$; n = 76) or mud constituents ($r^2 = 0.61$; n = 76) (Figure 2), indicating that the TOC content could be mainly dependent on the sediment grain size [*Zhu et al*., 2011].

3.2. Distribution and Compositions of PAHs

[13] The total concentration of the 16 PAHs in the sediments varied from 38 to 308 ng/g (dry weight), with a mean of 118 ng/g (Figure 3 and Table S2). Comparing to other large estuarine-coastal systems, the PAH concentration levels in YREMA (38–308 ng/g) and MZCMA (42–244 ng/g) were slightly lower than the Pearl River Delta (138–1100 ng/g) [*Chen et al*., 2006], the Bay of Bengal (25–1081 ng/g) [*Guzzella et al*., 2005], and the Nile Estuary (3.49–2010 ng/g) [*Barakat et al*., 2011], but they were comparable to the Mississippi River Delta [*Mitra and Bianchi*, 2003] and higher than the Yellow River Estuary [*Qin et al*., 2011]. This is not surprising, because the middle and lower reaches of the Yangtze are one of the most developed and populated regions of China. Spatially, in the stretch between the YRE and the south of Hangzhou Bay, PAHs were high at 190–308 ng/g. The lowest concentrations were north of the YRE at <70 ng/g (Figure 3). Modern YRE is the main accumulation area of the Yangtze-derived sediments, therefore high PAHs is to be expected; however, this was not the case, possibly due to the large accumulation of fluvial terrigenous sediments, which dilutes the pollutants in YREMA. PAH concentrations in north MZCMA were significantly higher than those in the south. This is in contrast to the spatial variation of the sediment grain sizes or TOC contents, suggesting that sediment sorting during deposition and TOC could not have played an important role in controlling the distribution of PAHs in this area.

[14] The 16 PAHs are generally grouped according to their source characteristics into 2 + 3 ring, 4 ring, and 5 + 6 ring for discussion. In Figure 3, high 2 + 3 ring PAH concentrations (31–171 ng/g, mean 89 ng/g) were observed in YREMA and northern MZCMA (29 ~ 30°N), constituting 42–83% (mean 60 ± 13%; n = 33) of the total 16 PAHs, while in the middle and southern MZCMA (south to 29°N), it was below 100 ng/g (45 ng/g mean) and 20–65%

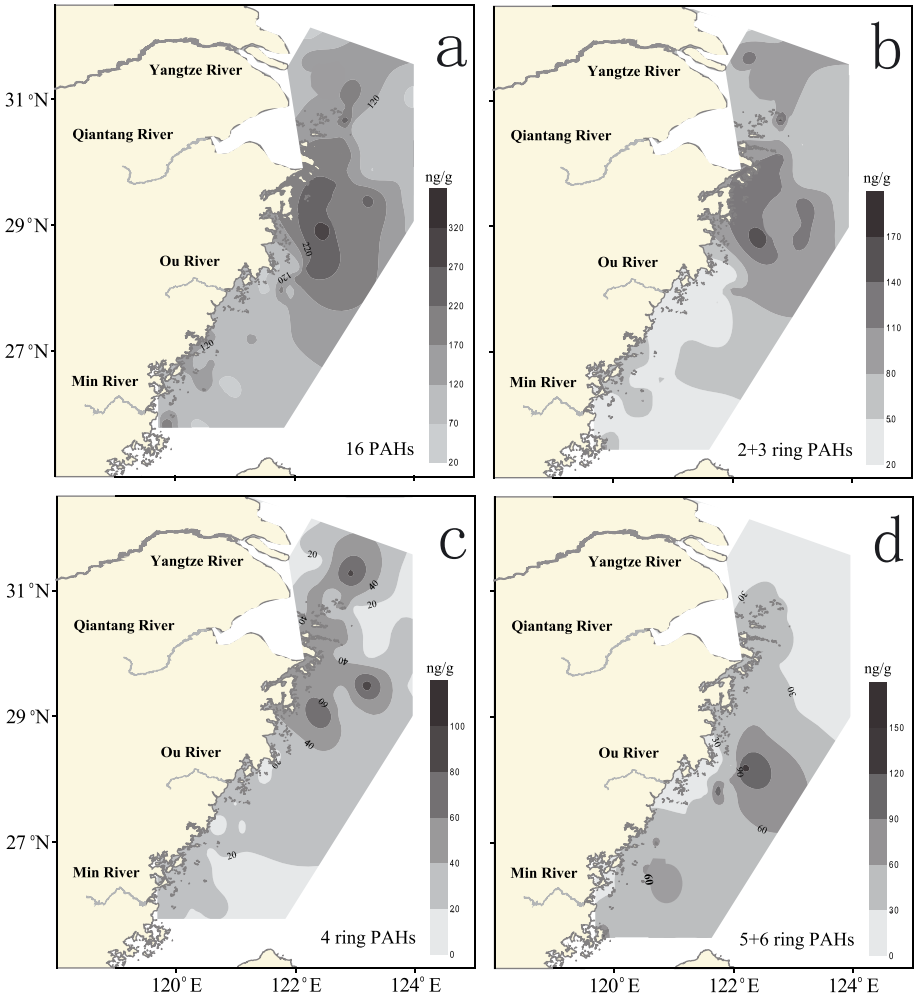

Figure 3. Distribution of concentrations of (a) 16 PAHs, (b) 2 + 3 ring PAHs, (c) 4-ring PAHs, and (d) 5 + 6 ring PAHs in the sediments of the Yangtze estuarine-inner shelf of ECS.

of the total 16 PAHs (mean 40 ± 12%; n = 43). In contrast, high levels of the 5 + 6 ring PAHs were observed in the middle and southern MZCMA, and they also had higher proportions (17–64%; mean 37 ± 11%; n = 43) than those of YREMA and northern MZCMA (3–31%; mean 19 ± 9%; n = 33) (Figure 3). These results revealed a marked composition variation in 16 PAHs along the ECS inner shelf from YREMA to MZCMA (Figure 3). In general, 2 + 3 ring PAHs (low-molecular-weight (LMW) PAHs) are mainly from petrogenic sources, while the high-temperature pyrogenic process generates mainly 4–6-ring PAHs (high-molecular-weight (HMW) PAHs) [*Soclo et al*., 2000; *Mai et al*., 2003]. In this study, high ratios of LMW to HMW PAHs (>2) were found in most samples from YREMA, suggesting a significant contribution from petrogenic sources.

3.3. Deposition Flux of PAHs

[15] The mass inventories of the PAHs were estimated according to *Tolosa et al*. [1996], *Chen et al*. [2006], and *Lin et al*. [2009]. The study area was divided into 76 homogeneous sectors, with the sampling sites located in the center of their respective sectors. The mass inventory (I) was calculated according to the following equation:

$$I = \sum_{i=1}^{76} CiAidpi \quad (3)$$

where *Ci* is the PAH concentration in the sediment sample, *Ai* is the water surface area (see supporting information), d is the recommended sediment dry density of 1.2 g/cm^3 for this area according to *Liu et al*. [2007], and pi is sedimentary rate for each sample site after *DeMaster et al*. [1985], *Huh and Su* [1999], and *Liu et al*. [2006, 2007] (Figure S1). The total deposition flux estimated for the approximately 80,000 km^2 of the mud areas in the Yangtze estuarine-inner shelf was 152 t/yr. *Qin et al*. [2011] estimated the deposition flux of the 16 PAHs in the southern Bohai Sea to be 36 t/yr (43,000 km^2). *Chen et al*. [2006] estimated that 40 t/yr of PAHs were deposited in 23,000 km^2 around the Pearl River Estuary and northern South China Sea. The deposition flux of land-based PAHs in the Yangtze estuarine-inner shelf of ECS (152 t/yr) is much higher than other continental shelves around the world, such as the Gulf of Mexico and Mediterranean Sea (Table 1). This is likely caused by the huge drainage basin of the Yangtze, which supports the livelihood of 400 million people. It is unmatched by any other rivers in China, and perhaps in the world.

Table 1. Annual Deposition Flux of the 16 PAHs in the Yangtze Estuarine-Inner Shelf of ECS and Other Estuarine/Coastal Areas in the World

Locations	Area (km^2)	Deposition Flux (t/yr)	References
Southern Bohai Sea	43,000	36.6	*Qin et al*. [2011]
Yellow Sea	70,000	15	Our unpublished data
Pearl River Estuary and the northern South China Sea	23,000	40	*Chen et al*. [2006]
Northwestern Mediterranean	280,000	60	*Tolosa et al*. [1996]
Mediterranean Sea	850,000	182	*Lipiatou et al*. [1997]
The Gulf of Mexico	1600,000	3.4 ± 1.1*	*Mitra and Bianchi*, 2003
The inner shelf of ECS	80,000	152	This study

*BghiP

[16] *Wang et al*. [2007] reported that the flux of 16 PAHs from the Yangtze into ECS is 232 t/yr, and it is only 11 t/yr from the Qiantang (Figure 4). Besides riverine runoff, atmospheric deposition is another of the important PAH inputs of the oceans. The atmospheric deposition flux of PAHs can be roughly estimated. *Deng et al*. [2006] estimated the deposition flux of dusts of the Yangtze Delta coast in 2000–2003 to be 11.1 g/m^2 yr, and the background 16 PAH concentration of these dusts was reported by *Ren et al*. [2006] to be ~20 μg/g. Thus, the annual atmospheric deposition of the 16 PAHs is ~150 t/yr for the entire ECS, an area of 700,000 km^2 (Figure 4), suggesting that ~38% of the total annual input to ECS ended up in the sediments of the Yangtze estuarine-inner shelf mud areas. More importantly, the deposition flux of 16 PAHs was observed to decrease from YREMA southward to MZCMA, suggesting that the Yangtze was the predominant PAH input.

3.4. Fate of PAHs

3.4.1. Correlation Between PAHs and TOC

[17] Because of their relative low solubility and hydrophobic nature, PAHs usually correlate well with TOC in sediments and this relationship has been used to determine the fate of PAHs in the environment [*Wang et al*., 2001; *Boonyatumanond et al*., 2006]. In this study, however, the correlation between PAHs and TOC varied, even though the latter correlated well with sediment grain size, as shown in Figure 2. For example, in YREMA and MZCMA, the correlation between the LMW PAHs and TOC was poor, while for the HMW PAHs and TOC, it was good only in YREMA, but very poor in MZCMA (Figure 5). This was also observed in other estuarine-coastal environments. *Mai et al*. [2003] reported that this is frequently observed in the estuarine-coastal sediments where the PAH and TOC sources are heterogeneous, and *Cai et al*. [2008] noted this is to be expected in an environment where there is a continuous and extensive PAH input.

[18] One of the factors influencing the relationship between PAHs and TOC is the source characteristics. In our case, PAHs are multiple-sourced with the main origins from the exhausts of combustion processes in the drainage area, as well as the huge and continuous output from the Yangtze, while planktonic organic matter in the inner shelf is also an important TOC contributor besides terrestrial input from the Yangtze [*Zhu et al*., 2011]. On top of this, the resuspension of the surface sediments triggered by the East Asian monsoon is strong. During this process, both concentrations and composition of TOC and PAHs will significantly change in the individual nature [*McGroddy et al*., 1995; *Chiou et al*., 1998; *Rockne et al*., 2002; *Cornelissen et al*., 2005]. The LMW PAHs (relatively less hydrophobic) is still readily depleted from those fine particles during extensive physical disturbance [*Mitra et al*., 1999]. This suggests that the dynamics of the waters in our study area is complicated and the various controlling factors could and would impact the equilibrium between the PAHs and TOC in the water and the sediments along the transport path.

3.4.2. Compositional Variations of PAHs Revealed by PCA and PMF

[19] The composition of the PAHs in marine sediments is dependent on many factors, such as physiochemical properties, source characteristics, and environmental conditions. In

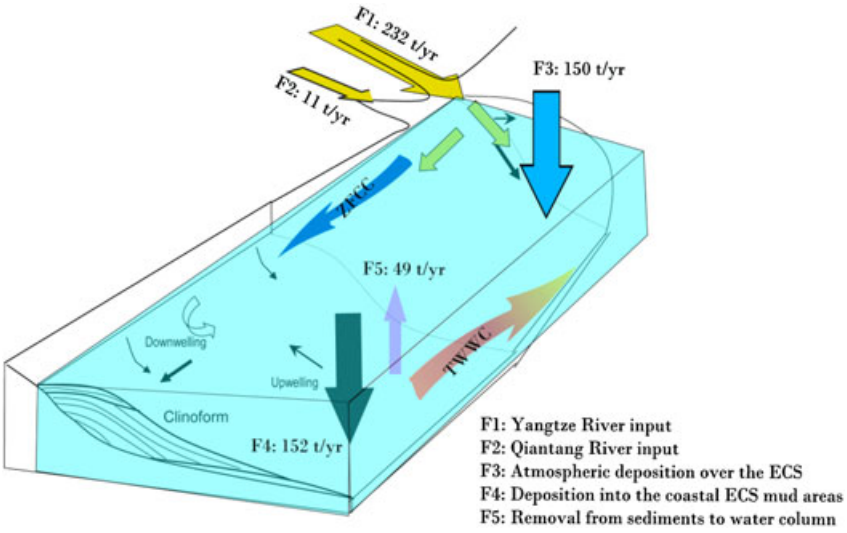

Figure 4. General fluxes of 16 PAHs in the Yangtze estuarine-inner shelf of ECS (the down-welling, upwelling and coastal clinoform mud were redrawn from *Liu et al*. [2006]; data of F1 and F2 is from *Wang et al*. [2007]).

the majority of the studies, evaluation of the spatial variation of PAH composition was based mainly on the aromatic ring numbers (e.g., 2 + 3 ring, 4 ring, and 5 + 6 ring). In this work, we introduced PMF as a novel method to give more objective classification to study the factors that influence the spatial variation, composition, and fate of PAHs.

[20] PCA identified the first three PCs based on factor loadings, which accounted for 91% of the total variance. PC1, explaining 50% of the total variance, is heavily weighted by PHE, which is attributable to petrogenic origins. PC2, contributing 25% of the total variance, has significant positive loadings of HMW PAHs. PC3, which explains 11% of the total variance, is mainly NAP, FL, and PHE. The PCA score plot reflected a gradient of decreasing PHE compositions from YREMA to the enrichment of HMW PAHs in MZCMA (Figure 6).

[21] PCA can only provide qualitative information about the contribution of the various factors to the PAHs data; however, to obtain the contribution of every sample, the PMF modeling is required. A 3-factor solution was also adopted for the PMF analysis similar to the PCA model. The factor profiles of the 3-factor solution of PMF and PCA are in Figure 7. PMF and PCA gave similar loadings for the same factors with similar compound profiles (Figure 7). Factor 1 is dominated by PHE, which is believed to be related to crude oil or refined petroleum releases and their degradation products, suggesting petrogenic sources in river runoff [*Zakaria et al*., 2002; *Mai et al*., 2003]. Factor 2 is predominately HMW PAHs because of their low solubility [*Lipiatou et al*., 1993; *Dachs et al*., 1996; *Tsapakis et al*., 2003]. Factor 3 is heavily weighted on LMW PAHs and moderately on the 4-ring PAHs, and it overlaps considerably factor 1, which contains mostly LMW, semivolatile PAHs. Figure 8 shows the PMF-based concentrations and contribution variations of the three factors of the data set. Factor 1, explaining 49% of the measured PAHs, is a major contributor of the PAHs in YREMA. There is a clear decreasing contribution of factor 1 from the YRE to the southern MZCMA (Figure 8). In contrast, factor 2, explaining 29% of the measured PAHs, is opposite to factor 1 in trend. Factor 3, accounting for 21% of the measured PAHs, is similar to factor 1's trend.

3.4.3. Partitioning and Fate of PAHs

[22] The 16 PAH deposition fluxes calculated based on PMF factor 1 concentrations were 48 t/yr for YREMA and 22 t/yr for MZCMA (Figure 8b and Tables S4 and S5). The sedimentation rate at YREMA is much higher and thus is more rapid than MZCMA [*DeMaster et al*., 1985; *Huh and Su*, 1999; *Liu et al*., 2006] (Figure S1), suggesting that this process would retain more of LMW PAHs in the bottom sediments in YREMA. Most sediment-associated PAHs in the summer are trapped in YREMA due to the blocking effect of the northbound TWWC and ZFCC, and they are resuspended by the winter East Asian monsoon storms, and are transported by the southbound ZFCC to MZCMA [*Guo et al*., 2007; *Liu et al*., 2006, 2007]. LMW PAHs have aqueous solubility over 1.0 and their octanol-water partition coefficients (log Kow) range from 3.37 to 4.57, which are orders of magnitude different from HMW PAHs [*Mackay et al*., 1992]. In comparison, the LMW PAHs in the particles, owing to their relatively high water solubility and low K_{ow} values, are more readily released into the water column than HMW PAHs [*Chiou et al*., 1998; *Latimer et al*., 1999; *Mitra et al*., 1999; *Berrojalbiz et al*., 2011]. *Feng et al*. [2007] found that the LMW PAHs from resuspended fine particles are rapidly released into the overlying water. Therefore, the source characteristics (with relatively high proportion of LMW PAHs, 42–83% with an average of 66%) in YREMA, and the properties of LMW PAHs themselves (low K_{ow} and high water solubility) could induce a depletion of LMW PAHs during resuspension and transport from the north to the south triggered by the East Asian monsoon.

[23] In contrast, the 16 PAH deposition fluxes identified by factor 2 were similar for YREMA (17 t/yr) and MZCMA (21 t/yr) (Figure 8c and Tables S4 and S5).

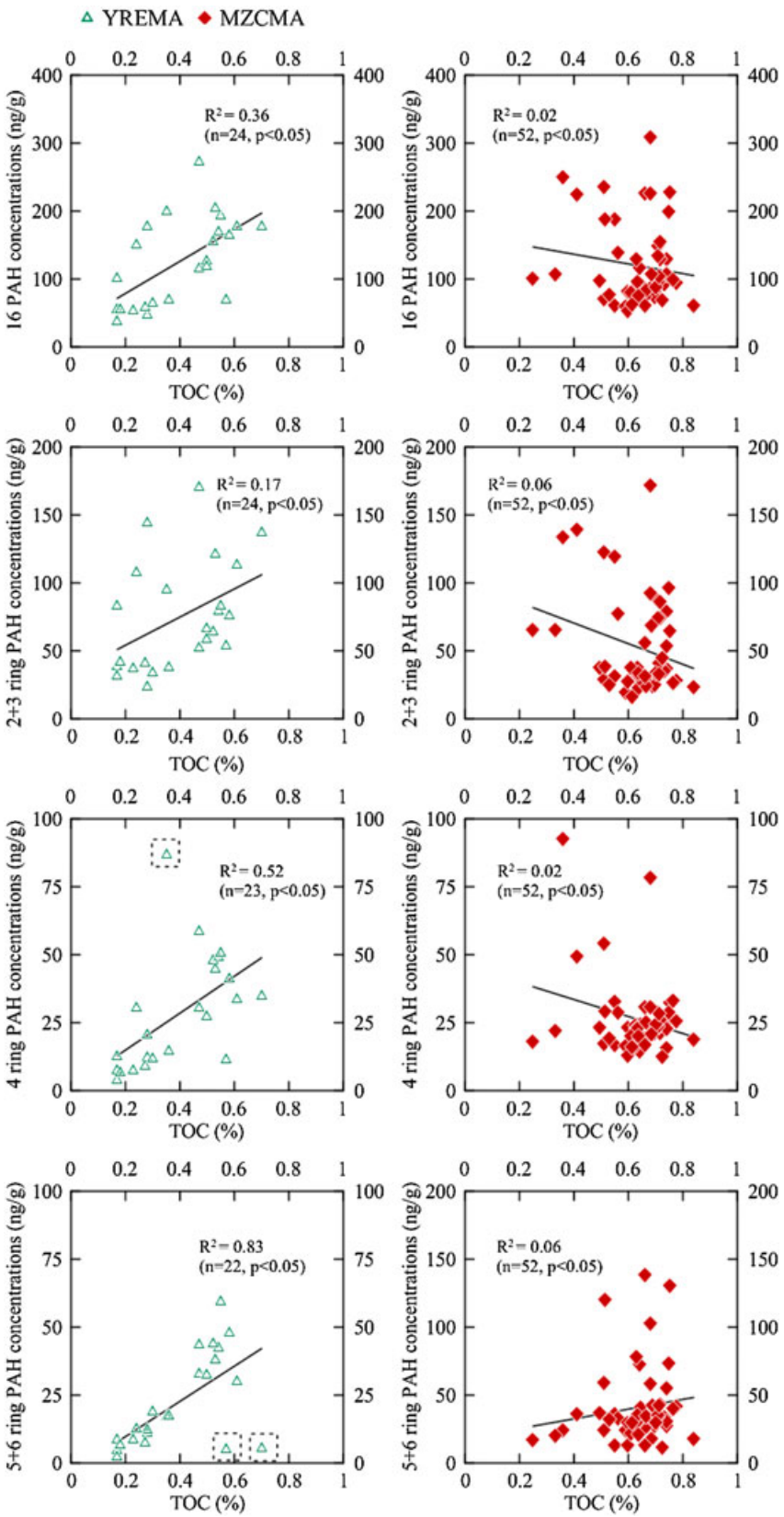

Figure 5. Correlations of TOC with 16 PAHs, 2 + 3 ring PAHs, 4-ring PAHs, and 5 + 6 ring PAHs in sediments of YREMA and MZCMA.

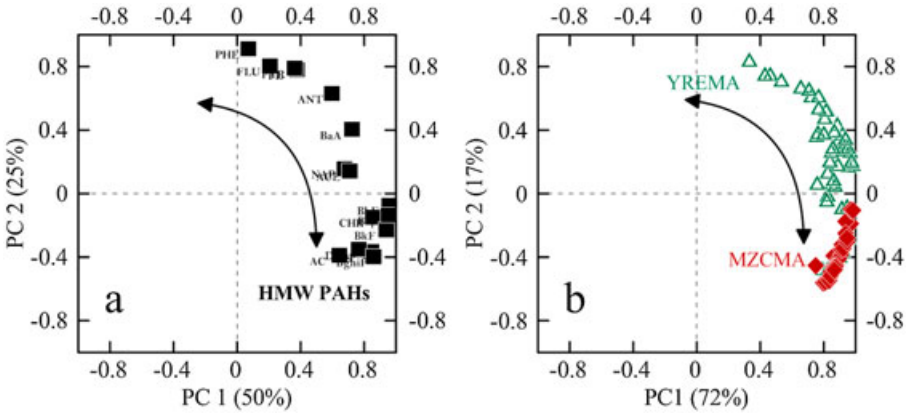

Figure 6. Factor scores (a) and factor loadings (b) of the PCA model of the 16 PAHs from 76 sediment samples in the Yangtze estuarine-inner shelf of ECS.

Factor 2 is characterized by HMW PAHs, mostly in the particulate phase. They are less degradable in the water column, and are thus more effectively transported and eventually incorporated into the sediments [*Dachs et al*., 1996; *Berrojalbiz et al*., 2011; *Lin et al*., 2011]. This suggests that the HMW PAHs were enriched during transport and redeposition. Although the HMW PAH composition along the transport path varied much less than that of the LMW PAHs, variations still existed in the HMW PAH molecular diagnostic ratio pairs. Generally, the ratio of BaA/(BaA + Chr) is reported to be <0.2 for petrogenic source and >0.35 for pyrogenic source, while between 0.2 and 0.35 for a mixed source of petroleum and combustion origins; Flu/(Flu + Pyr) <0.4, $0.4-0.5$, and >0.5 and IP/(IP + BghiP) <0.2, $0.2-0.5$, and >0.5 indicate PAHs from petrogenic origin, liquid fossil fuel combustion, and coal/wood combustion, respectively [*Yunker et al*., 2002]. As shown in Figure 9, the ratios of FLU/(FLU + PYR), BaA/(BaA + CHR), and IP/(IP + BghiP) decreased from YREMA to MZCMA, and the decrease was more pronounced in BaA/(BaA + CHR) and FLU/(FLU + PYR). Two explanations can be offered for this change: 1) a source shift from pyrogenic to petrogenic along the transport path and 2) the more degradation of selected congeners during the transport. PYR has been reported to be more persistent than FLU in the environment [*Yu et al*., 2005], and *Zhang et al*. [2005] found that BaA/(BaA + CHR) and IP/(IP + BghiP) gradually decreased from soil to sediments, suggesting faster degradation of BaA and IP than CHR and BghiP. With no obvious additional sources along the transport path, the second explanation is the more acceptable one. Furthermore, the more significant decreases of FLU/(FLU + PYR) and BaA/(BaA + CHR) suggest that the compositions of the 4-ring PAHs are more susceptible to changes during transport than the

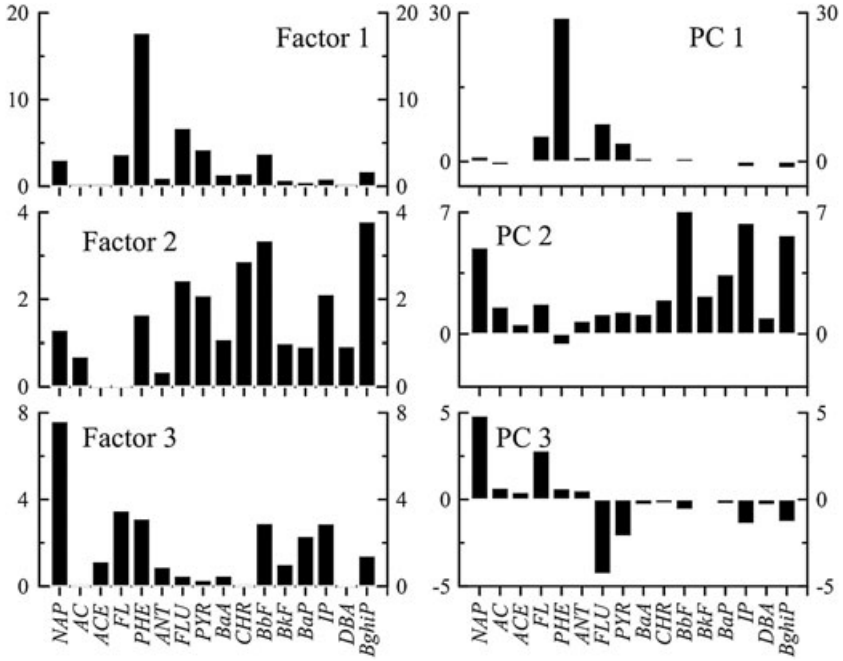

Figure 7. Factor profiles (PC loadings) obtained from the PMF and PCA analysis of PAH concentrations in sediments of the Yangtze estuarine-inner shelf of ECS.

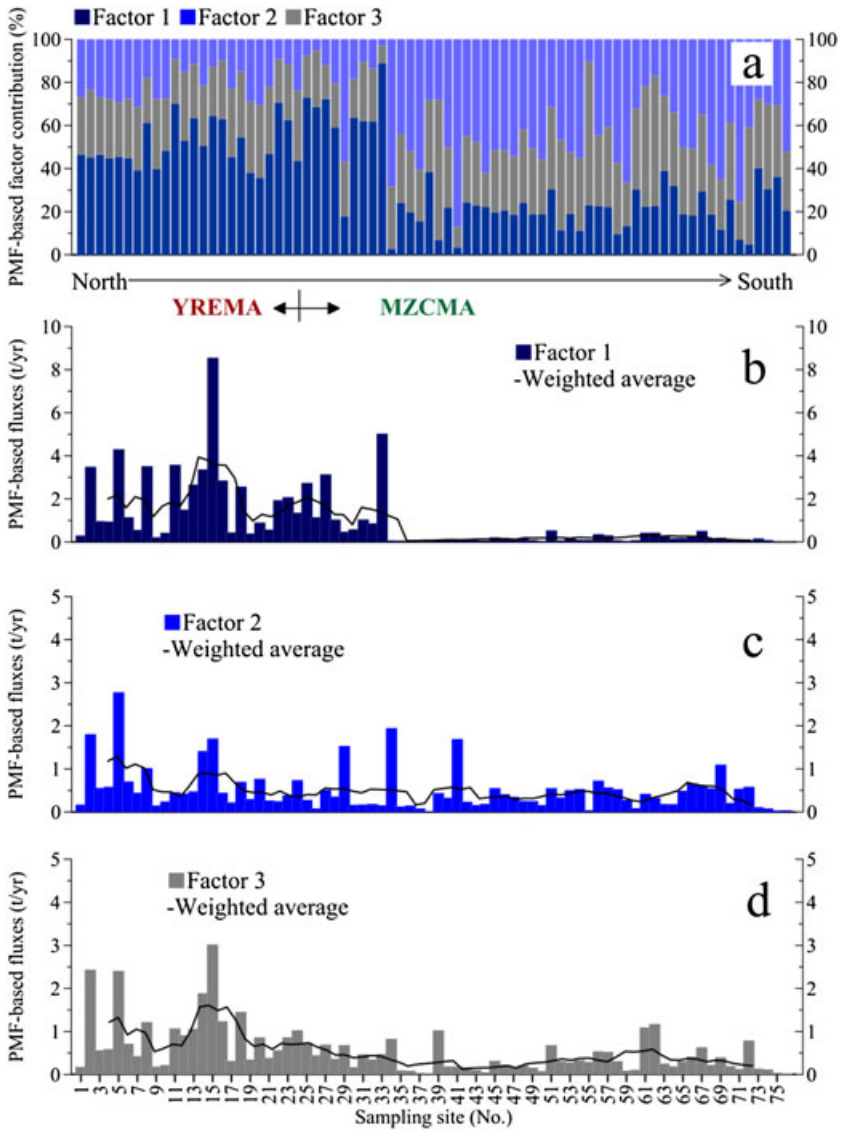

Figure 8. Stacked histograms showing the variations of contribution concentration of factors 1, 2, and 3 (a) and flux of 16 PAHs contributed by factors 1 (b), 2 (c), and 3 (d) in sediments estimated by the PMF model.

6-ring ones, most likely due to the molecular weights, thus not related to the sources.

[24] For factor 3, the PMF estimated flux was higher in YREMA (23 t/yr) than MZCMA (17 t/yr) similar to factor 1 (Figure 8d and Tables S4 and S5), but factor 3 had higher loadings of NAP and FL. Factor 3 also suggested that there was a loss of NAP and FL during the resuspension and transport of the sediments.

[25] Another angle to substantiate the loss of LMW PAHs, such as NAP, FL, and PHE, is to estimate the relative fluxes of these compounds. Assuming that factors 1 and 3 (mainly consisted of LMW PAHs) PAHs behaved similarly during resuspension and transport and were as stable as those of factor 2 (HMW PAHs), the total deposition flux of the factor 1 and 3 PAH compounds in MZCMA would be ~88 t/yr by assuming the deposition flux ratio of (factor 1 + factor 3)/factor 2 is "constant" as in YREMA. However, this factor 1 and 3 PAH deposition flux was actually only ~39 t/yr. Therefore, the loss of LMW PAHs (mainly NAP, FL, and PHE) during transport would be 49 t/yr. Considering that the deposited PAHs in the coastal ECS mud areas are mainly from the Yangtze, and the sediments and the associated PAHs in MZCMA are dominantly from the resuspended YREMA sediments, this estimation looks reasonable based on the uncertainties in the assumptions. This supports that the LMW PAHs released by the resuspension and transport of the bottom sediments driven by the winter East Asian monsoon could be an important secondary PAH source of the water in ECS. Furthermore, because of the relatively high solubility of these LMW compounds, the PAHs selectively depleted are more readily retained in the water columns and can therefore be efficiently uptaken by aquatic organisms, or even released to atmosphere [*Arzayus et al.*, 2001; *Tsapakis et al.*, 2006; *Berrojalbiz et al.*, 2011], suggesting that these depleted PAHs may also have

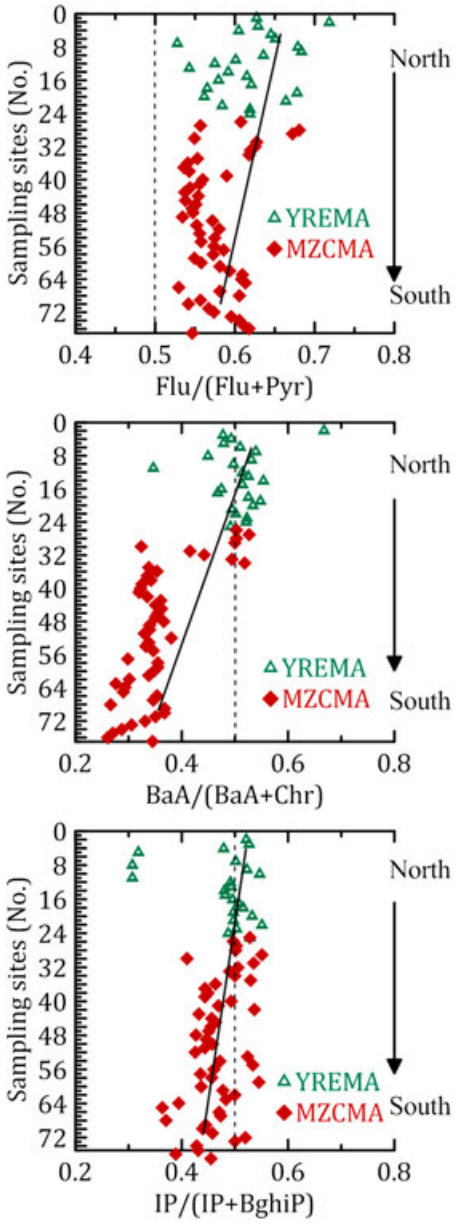

Figure 9. Parent PAH ratios vs. numbers of sampling sites in the Yangtze estuarine-inner shelf of ECS.

implications to the organic contaminant cycle and biogeochemical effect on the ecosystems in ECS.

4. Conclusions

[26] The 16 PAH data of the 76 surface sediment samples in two mud areas of the ECS inner shelf allowed the estimation of the total deposition flux of these PAHs to be 152 t/yr, representing ~38% of the total annual input of the PAHs into the ECS. The ECS inner shelf is the largest reservoir of land-based PAHs in the East Asian marginal seas.

[27] Correlation between HMW PAHs and TOC shifted from good in YREMA to poor in MZCMA, suggesting that the equilibrium between PAHs and TOC in MCZMA has not been reached, probably due to the different sorption/desorption ability during the resuspension and transport of the sediments.

[28] ECS is much influenced by ocean currents and waves induced by the East Asian monsoon, which, in turn, play important roles in the resuspension and transport of the sediments at the YRE. These conditions, together with the difference in the physical and chemical properties of the PAHs and the sediments, caused the partitioning of these compounds (i.e., the selective depletion of LMW PAHs and the enrichment of HMW PAHs from the north of the inner shelf to the south), as observed in the PCA and PMF analyses.

[29] **Acknowledgments.** This work was supported by the Natural Science Foundation of China (NSFC) (41076015, 40776062, 41103046, and 41176085) and, in part, by the State Oceanic Administration (SOA), China (GY02-2012G08). The authors are most grateful to Ming Fang of the Hong Kong University of Science and Technology for his invaluable advices in finalizing the manuscript. The authors wish to thank the crew of *R/V Dong Fang Hong 2* of the Ocean University of China and the R/V Kan 407, for collecting the sediment samples. The anonymous reviewers and associate editor should be sincerely appreciated for their constructive comments that greatly improved this study.

References

Arzayus, K. M., R. M. Dickhut, and E. A. Canuel (2001), Fate of atmospherically deposited polycyclic aromatic hydrocarbons (PAHs) in Chesapeake Bay, *Environ. Sci. Technol.*, *35*(11), 2178–2183, doi:10.1021/es001672s.

Barakat, A. O., A. Mostafa, T. L. Wade, S. T. Sweet, and N. B. El Sayed (2011), Distribution and characteristics of PAHs in sediments from the Mediterranean coastal environment of Egypt, *Mar. Pollut. Bull.*, *62*(9), 1969–1978, doi:S0146-6380(02)00002-5/j.marpolbul.2011.06.024.

Berrojalbiz, N., J. Dashes, M. J. Ojeda, M. C. Valle, J. Castro-Jimenez, J. Wollgast, M. Ghiani, G. Hanke, and J. M. Zaldivar (2011), Biogeochemical and physical controls on concentrations of polycyclic aromatic hydrocarbons in water and plankton of the Mediterranean and Black seas, *Global Biogeochem. Cycles*, *25*, GB4003, doi:10.1029/2010GB003775.

Bianchi, T. S., and M. A. Allison (2009), Large-river delta-front estuaries as natural "recorders" of global environmental change, *Proc. Natl. Acad. Sci. U. S. A.*, *106*, 8085–8092, doi:10.1073/pnas.0812878106.

Boonyatumanond, R., G. Wattayakorn, A. Togo, and H. Takada (2006), Distribution and origins of polycyclic aromatic hydrocarbons (PAHs) in riverine, estuarine, and marine sediments in Thailand, *Mar. Pollut. Bull.*, *52*(8), 942–956, doi:s0304-4203(02)00132-9/j.marpolbul.2005.12.015.

Cai, Q. Y., C. H. Mo, Q. T. Wu, A. Katsoyiannis, and Q. Y. Zeng (2008), The status of soil contamination by semi-volatile organic chemicals (SVOCs) in China: A review, *Sci. Total Environ.*, *389*(2–3), 209–224, doi:s0304-4203(02)00132-9/j.scitotenv.2007.08.026.

Chen, S. J., X. J. Luo, B. X. Mai, G. Y. Sheng, J. M. Fu, and E. Y. Zeng (2006), Distribution and mass inventories of polycyclic aromatic hydrocarbons and organochlorine pesticides in sediments of the Pearl River Estuary and the Northern South China Sea, *Environ. Sci. Technol.*, *40*(3), 709–714, doi:10.1021/es052060g.

Chiou, C. T., S. E. McGroddy, and D. E. Kile (1998), Partition characteristics of polycyclic aromatic hydrocarbons on soils and sediments, *Environ. Sci. Technol.*, *32*(2), 264–269, doi:10.1021/es970614c.

Chu, Z. X., S. K. Zhai, X. X. Lu, J. P. Liu, J. X. Xu, and K. H. Xu (2009), A quantitative assessment of human impacts on decrease in sediment flux from major Chinese rivers entering the western Pacific Ocean, *Geophys. Res. Lett.*, *36*, L19603, doi:10.1029/2009GL039513.

Cornelissen, G., Ö. Gustafsson, T. D. Bucheli, M. T. O. Jonker, A. A. Koelmans, and P. C. M. van Noort (2005), Extensive sorption of organic compounds to black carbon, coal, and kerogen in sediments and soils: Mechanisms and consequences for distribution, bioaccumulation, and biodegradation, *Environ. Sci. Technol.*, *39*(18), 6881–6895, doi:10.1021/es050191b.

Dachs, J., J. M. Bayona, S. W. Fowler, J. C. Miquel, and J. Albaiges (1996), Vertical fluxes of polycyclic aromatic hydrocarbons and organochlorine compounds in the western Alboran Sea (southwestern Mediterranean), *Mar. Chem.*, *52*, 75–86, doi:SSDI 0304-4203(95)00084-4.

DeMaster, D. J., B. A. McKee, C. A. Nittrouer, J. C. Qian, and G. D. Chen (1985), Rates of sediment accumulation and particle reworking based on radiochemical measurements from continental shelf deposits in the East China Sea, *Cont. Shelf Res.*, *4*(1–2), 143–158, doi:s0304-4203(02)00132-9/0278-4343(85)90026-3.

Deng, B., J. Zhang, and Y. Wu (2006), Recent sediment accumulation and carbon burial in the East China Sea, *Global Biogeochem. Cycles*, *20*, GB3014, doi:10.1029/2005GB002559.

Feng, J., Z. Yang, J. Niu, and Z. Shen (2007), Remobilization of polycyclic aromatic hydrocarbons during the resuspension of Yangtze River sediments using a particle entrainment simulator, *Environ. Pollut.*, *149*(2), 193–200, doi:s0304-4203(02)00132-9/j.envpol.2007.01.001.

Greenfield, B. K., and J. A. Davis (2005), A PAH fate model for San Francisco Bay, *Chemosphere*, *60*(4), 515–530, doi:10.1016/j.chemosphere.2005.01.004.

Guo, Z., T. Lin, G. Zhang, M. Zheng, Z. Zhang, Y. Hao, and M. Fang (2007), The sedimentary fluxes of polycyclic aromatic hydrocarbons in the Yangtze River Estuary coastal sea for the past century, *Sci. Total Environ.*, *386*(1–3), 33–41, doi:10.1016/j.scitotenv.2007.07.019.

Guzzella, L., C. Roscioli, L. Viganò, M. Saha, S. K. Sarkar, and A. Bhattacharya (2005), Evaluation of the concentration of HCH, DDT, HCB, PCB, and PAH in the sediments along the lower stretch of Hugli estuary, West Bengal, northeast India, *Environ. Inter.*, *31*(4), 523–534, doi:10.1016/j.envint.2004.10.014.

Hu, L. M., Z. G. Guo, J. L. Feng, Z. S. Yang, and M. Fang (2009), Distributions and sources of bulk organic matter and aliphatic hydrocarbons in surface sediments of the Bohai Sea, China, *Mar. Chem.*, *113*, 197–211, doi:10.1016/j.marchem.2009.02.001.

Hu, L. M., T. Lin, X. F. Shi, Z. S. Yang, H. J. Wang, G. Zhang, and Z. G. Guo (2011), The role of shelf mud depositional process and large river inputs on the fate of organochlorine pesticides in sediments of the Yellow and East China seas, *Geophys. Res. Lett.*, *38*(3), L03602, doi:10.1029/2010gl045723.

Huh, C. A., and C. C. Su (1999), Sedimentation dynamics in the East China Sea elucidated from ^{210}Pb, ^{137}Cs, and ^{239,240}Pu, *Mar. Geol.*, *160*, 183–196, doi:10.1016/S0025-3227(99)00020-1.

Latimer, J. S., W. R. Davis, and D. J. Keith, (1999), Mobilization of PAHs and PCBs from in-place contaminated marine sediments during simulated resuspension events, *Estuar. Coast. Shelf Sci.*, *49*, 577–595, doi:10.1006/ecss.1999.0516.

Lima, A. L., J. W. Farrington, and C. M. Reddy (2005), Combustion-derived polycyclic aromatic hydrocarbons in the environment—a review, *Environ. Forensics*, *6*, 109–131, doi:10.1080/15275920590952739.

Lin, T., Z. H. Hu, G. Zhang, X. D. Li, W. H. Xu, J. H. Tang, and J. Li (2009), Levels and mass burden of DDTs in sediments from fishing harbors: The importance of DDT-containing antifouling paint to the coastal environment of China, *Environ. Sci. Technol.*, *43*(21), 8033–8038, doi:10.1021/es901827b.

Lin, T., L. M. Hu, Z. G. Guo, Y. W. Qin, Z. S. Yang, G. Zhang, and M. Zheng (2011), Sources of polycyclic aromatic hydrocarbons to sediments of the Bohai and Yellow Seas in East Asia, *J. Geophys. Res.*, *38*, L03602, doi:10.1029/2010GL045723.

Lipiatou, E., J. C. Marty, and A. Saliot (1993), Sediment trap fluxes of polycyclic aromatic hydrocarbons in the Mediterranean Sea, *Mar. Chem.*, *44*(1), 43–54, doi:10.1016/0304-4203(93)90005-9.

Lipiatou, E., et al. (1997), Mass budget and dynamics of polycyclic aromatic hydrocarbons in the Mediterranean Sea, *Deep-Sea Res. Part II: Topical Studies in Oceanography*, *44*(3–4), 881–905, doi:10.1016/s0967-0645(96)00093-8.

Liu, J. P., A. C. Li, K. H. Xu, D. M. Velozzi, Z. S. Yang, J. D. Milliman, and D. J. DeMaster (2006), Sedimentary features of the Yangtze River-derived along-shelf clinoform deposit in the East China Sea, *Cont. Shelf Res.*, *26*(17–18), 2141–2156, doi:10.1016/j.csr.2006.07.013.

Liu, J. P., K. H. Xu, A. C. Li, J. D. Milliman, D. M. Velozzi, S. B. Xiao, and Z. S. Yang (2007), Flux and fate of Yangtze River sediment delivered to the East China Sea, *Geomorphology*, *85*(3–4), 208–224, doi:10.1016/j.geomorph.2006.03.023.

Mackay, D., W. Y. Shiu, and K. C. Ma (1992), Illustrated Handbook of Physical-Chemical Properties and Environmental Fate for Organic Chemicals, *vol. II, Polynuclear Aromatic Hydrocarbons, Polychlorinated Dioxins, and Dibenzofurans*, Lewis, Chelsea, Mich.

Mai, B. X., J. M. Fu, G. Zhang, Z. Lin, Y. S. Min, G. Y. Sheng, and X. M. Wang (2001), Polycyclic aromatic hydrocarbons in sediments from the Pearl river and estuary, China: Spatial and temporal distribution and sources, *Appl. Geochem.*, *16*(11–12), 1429–1445, doi:10.1016/S0883-2927(01)00050-6.

Mai, B. X., S. H. Qi, E. Y. Zeng, Q. S. Yang, G. Zhang, J. M. Fu, G. Y. Sheng, P. A. Peng, and Z. S. Wang (2003), Distribution of polycyclic aromatic hydrocarbons in the coastal region off Macao, China: Assessment of input sources and transport pathways using compositional analysis, *Environ. Sci. Technol.*, *37*(21), 4855–4863, doi:10.1021/es034514k.

McGroddy, S. E., J. W. Farrington, and P. M. Gschwend (1995), Comparison of the in situ and desorption sediment-water partitioning of polycyclic aromatic hydrocarbons and polychlorinated biphenyls, *Environ. Sci. Technol.*, *30*(1), 172–177, doi:10.1021/es950218z.

Milliman, J. D., H. T. Shen, Z. S. Yang, and R. H. Mead (1985), Transport and deposition of river sediment in the Changjiang Estuary and adjacent continental shelf, *Cont. Shelf Res.*, *4*(1–2), 37–45, doi:10.1016/0278-4343(85)90020-2.

Mitra, S., T. M. Dellapenna, and R. M. Dickhut (1999), Polycyclic aromatic hydrocarbon distribution within Lower Hudson River estuarine sediments: Physical mixing vs sediment geochemistry, *Estuar., Coast. Shelf Sci.*, *49*(3), 311–326, doi:10.1006/ecss.1999.0502.

Mitra, S., and T. S. Bianchi (2003), A preliminary assessment of polycyclic aromatic hydrocarbon distributions in the lower Mississippi River and Gulf of Mexico, *Mar. Chem.*, *82*(3–4), 273–288, doi:10.1016/S0304-4203(03)00074-4.

Qin, Y. W., B. H. Zheng, K. Lei, T. Lin, L. M. Hu, and Z. G. Guo (2011), Distribution and mass inventory of polycyclic aromatic hydrocarbons in the sediments of the south Bohai Sea, China, *Mar. Pollut. Bull.*, *62*, 371–376, doi:10.1016/j.marpolbul.2010.09.028.

Ren, Y., Q. J. Zhang, and J. M. Chen (2006), Distribution and source of polycyclic aromatic hydrocarbons (PAHs) on dust collected in Shanghai, *People's Republic of China. Bull. Environ. Contam. Toxicol.*, *76*(3), 442–449, doi:10.1007/s00128-006-0941-y.

Rockne, K. J., L. M. Shor, L. Young, G. L. Taghon, and D. S. Kosson (2002), Distributed sequestration and release of PAHs in weathered sediment: The role of sediment structure and organic carbon properties, *Environ. Sci. Technol.*, *36*(12), 2636–2644, doi:10.1021/es015652h.

Soclo, H. H., P. Garrigues, and M. Ewald (2000), Origin of polycyclic aromatic hydrocarbons (PAHs) in coastal marine sediments: Case studies in Cotonou (Benin) and Aquitaine (France) areas, *Mar. Pollut. Bull.*, *40*(5), 387–396, doi:10.1016/s0025-326x(99)00200-3.

Tolosa, I., J. M. Bayona, and J. Albaiges (1996), Aliphatic and polycyclic aromatic hydrocarbons and sulfur/oxygen derivatives in Northwestern Mediterranean sediments: Spatial and temporal variability, fluxes, and budgets. *Environ. Sci. Technol.*, *30*, 2495–2503, doi:10.1021/es950647x.

Tsapakis, M., E. G. Stephanou, and I. Karakassis (2003), Evaluation of atmospheric transport as a nonpoint source of polycyclic aromatic hydrocarbons in marine sediments of the Eastern Mediterranean, *Mar. Chem.*, *80*(4), 283–298, doi:10.1016/s0304-4203(02)00132-9.

Tsapakis, M., M. Apostolaki, S. Eisenreich, and E. G. Stephanou (2006), Atmospheric deposition and marine sedimentation fluxes of polycyclic aromatic hydrocarbons in the Eastern Mediterranean Basin, *Environ. Sci. Technol.*, *40*(16), 4922–4927, doi:10.1021/es060487x.

Wang, H. J., Y. Saito, Y. Zhang, N. S. Bi, X. X. Sun, and Z. S. Yang (2011), Recent changes of sediment flux to the western Pacific Ocean from major rivers in East and Southeast Asia, *Earth-Sci. Rev.*, *108*, 80–100, doi:10.1016/j.earscirev.2011.06.003.

Wang, J. Z., Y. F. Guan, H. G. Ni, X. L. Luo, and E. Y. Zeng (2007), Polycyclic aromatic hydrocarbons in riverine runoff of the Pearl River Delta (China): Concentrations, fluxes, and fate, *Environ. Sci. Technol.*, *41*(16), 5614–5619, doi:10.1021/es070964r.

Wang, X. C., Y. X. Zhang, and R. F. Chen (2001), Distribution and partitioning of polycyclic aromatic hydrocarbons (PAHs) in different size fractions in sediments from Boston Harbor, United States, *Mar. Pollut. Bull.*, *42*, 1139–1149, doi:10.1016/S0025-326X(01)00129-1.

Yang, Z. S., H. J. Wang, Y. Saito, J. D. Milliman, K. H. Xu, S. Q. Qiao, and G. Shi (2006), Dam impacts on the Changjiang (Yangtze) River sediment discharge to the sea: The past 55 years and after the Three Gorges Dam, *Water Resour. Res.*, *42*, W04407, doi:10.1029/2005WR003970.

Yu, K. S. H., A. H. Y. Wong, K. W. Y. Yau, Y. S. Wong, and N. F. Y. Tam (2005), Natural attenuation, biostimulation and bioaugmentation on biodegradation of polycyclic aromatic hydrocarbons (PAHs) in mangrove sediments, *Mar. Pollut. Bull.*, *51*(8–12), 1071–1077, doi:10.1016/j.marpolbul.2005.06.006.

Yunker, M. B., R. W. Macdonald, R. Vingarzan, R. H. Mitchell, D. Goyette, and S. Sylvestre (2002), PAHs in the Fraser River basin: A critical appraisal of PAH ratios as indicators of PAH source and composition, *Org. Geochem.*, *33*(4), 489–515, doi:10.1016/S0146-6380(02)00002-5.

Zakaria, M. P., H. Takada, S. Tsutsumi, K. Ohno, J. Yamada, E. Kouno, and H. Kumata (2002), Distribution of polycyclic aromatic hydrocarbons (PAHs) in rivers and estuaries in Malaysia: A widespread input of petrogenic PAHs, *Environ. Sci. Technol.*, *36*(9), 1907–1918, doi:10.1021/es011278+.

Zhang, X. L., S. Tao, W. X. Liu, Y. Yang, Q. Zuo, and S. Z. Liu (2005), Source diagnostics of polycyclic aromatic hydrocarbons based on species ratios: A multimedia approach, *Environ. Sci. Technol.*, *39*(23), 9109–9114, doi:10.1021/es0513741.

Zhu, C., Z. H. Wang, B. Xue, P. S. Yu, J. M. Pan, T. Wagner, and R. D. Pancost (2011), Characterizing the depositional settings for sedimentary organic matter distributions in the Lower Yangtze River-East China Sea shelf system, *Estuar., Coast. Shelf Sci.*, *93*(3), 182–191, doi:10.1016/j.ecss.2010.08.001.